05,08

The effect of platinum thickness on the magnetic properties of Pt/Co/CoO films

© M.A. Kuznetsova, A.A. Turpak, A.V. Prikhodchenko, N.N. Chernousov, A.G. Kozlov

Federal State Autonomous Educational Institution of Higher Education „Far Eastern Federal University“, Vladivostok, Russia

E-mail: kuznetcova.mal@dvfu.ru

Received March 6, 2025
Revised March 6, 2025
Accepted May 5, 2025

The paper presents the results of an experimental study of thin magnetic Pt/Co/CoO/Pt films fabricated by magnetron sputtering with varying thicknesses of the bottom Pt layer. The main focus is on investigating the influence of the Pt underlayer thickness on the magnetic properties and morphology of the studied films. Magnetic characteristics (coercivity and anisotropy field) were examined using a vibrating sample magnetometer. The domain wall propagation velocity depending on the Pt thickness was studied using a Kerr magneto-optical microscope, and the Dlozyashinsky-Moriya interaction (DMI) constant was calculated based on measurements of domain wall dynamics I. It was demonstrated that with an increase in the Pt sublayer, the average grain size increases, which leads to an increase in the coercive force, magnetic anisotropy and, and magnetic moment in the studied films. The results of this work may be useful for utilizing the Pt/Co/CoO/Pt system as a basis for developing new data storage devices with tailored magnetic properties for applications in spintronics.

Keywords: perpendicular magnetic anisotropy, cobalt oxidation, spin-orbit interaction, X-ray reflectometry, domain structure, Dzyaloshinskii-Moria interaction.

DOI: 10.61011/PSS.2025.07.61885.5HH-25

1. Introduction

Pt/Co/MO_x films, where M is an oxidized metal, are promising objects of spintronics studies [1], due to the possibility of implementing a wide range of boundary phenomena in them, in particular, perpendicular magnetic anisotropy, the Dzyaloshinskii-Moriya interaction (DMI) [2–5], exchange bias [6], etc. Such effects are of practical importance, for example, to implement track magnetic memory based on skyrmions [7,8], magnetic sensors [9], neuromorphic devices [10], etc.

Perpendicular magnetic anisotropy at the Pt/Co interface is induced as a result of hybridization between $5d$, a heavy metal with strong spin-orbit interaction and $3d$, a ferromagnetic [11,12], as well as contributions of magnetically elastic interface and magnetocrystalline anisotropy under the condition of coherent conjugation of Pt and Co grains [13], if these contributions are large enough to overcome the demagnetization energy [14,15]. Pt/Co/Pt films exhibit perpendicular magnetic anisotropy [16,17], the effect of spin-orbital moment transfer due to the spin Hall effect [18], DMI [19–21], etc. But their implementation requires a breaking of the symmetries of the Pt/Co and Co/Pt interfaces, for example, in Ref. [19], the upper and lower layers of Pt were obtained at different temperatures, and in Ref. [20] different argon pressure was used for sputtering.

Gd_2O_3 [2], MgO [3], Al_2O_3 [4], NiO [5] are usually used as an oxide material for thin magnetic layered structures such as Pt/Co/MO_x, as they allow inducing the above-mentioned effects. However, the effect of the CoO oxide layer on polycrystalline Co films remains poorly understood, although its presence makes it possible to change the magnetic structure by modifying the Co/CoO interface. The influence of the oxidation dose on the mechanism of oxide growth is shown in Refs. [22,23] as well as the increase in perpendicular magnetic anisotropy and DMI energy in thin epitaxial Pd/Co films. Moreover, CoO can be used as an antiferromagnetic layer to study exchange bias at low temperatures [6].

We study in our paper the effect of a heavy metal (platinum) sublayer on the structural and magnetic characteristics of ultrathin polycrystalline cobalt films in which the symmetry of the upper and lower interfaces was disrupted by partial controlled oxidation of the magnetic layer.

2. Experimental part

Polycrystalline magnetic films of Pt/Co/Co/Pt and Pt/Co/Pt were produced by magnetron sputtering in a high-vacuum system Omicron at room temperature. The base pressure of the main chamber was $P = 1 \cdot 10^{-8}$ Torr, pressure during sputtering $P = 1 \cdot 10^{-3}$ Torr; thermally oxidized Si(100) was used as substrates. The substrate was rotated at a speed of 40 rpm during the deposition process to prevent any growth anisotropy. The thickness of the Pt sublayer ranged from 3 to 15 nm, and the thickness of the ferromagnetic layer of Co was 1 nm. The thicknesses of the layers were selected in such a way as to induce

perpendicular magnetic anisotropy, as well as to allow partial oxidation of the ferromagnetic layer. Co oxidation was carried out in a separate chamber equipped with a gas flow sensor and a vacuum pressure gauge connected to the spray chamber. The exposure time in dry oxygen was 2 minutes at constant pressure of $P = 1 \cdot 10^{-3}$ Torr. All samples were coated with a protective layer of Pt (5 nm) to prevent further undesirable oxidation of the film.

The crystal structure of the films was analyzed using X-ray diffraction (XRD) methods. The structure and parameters of the interfaces were studied by X-ray reflectometry (XRR). X-ray spectra were measured using Kolibri diffractometer (Burevestnik, Russia) operating according to the Bragg-Brentano scheme, where ^{29}Cu with an excitation potential of $U_{\text{excit.}} = 8.86$ kV, radiation type $\alpha_1\ \alpha_2, \beta$ wavelength of $\lambda_{K_{\alpha\text{cp}}} = 0.154$ nm.

The surface morphology was studied using a scanning tunneling microscope (STM) installed in the Omicron Nanotechnology ultra-high vacuum complex, Germany.

The magnetic properties of the samples, such as the coercive force, the anisotropy field, and the magnetic moment, were investigated based on the measurement results of hysteresis loops obtained using a LakeShore vibration magnetometer 7410, USA.

The domain structure was visualized using an Evico-Magnetics magneto-optical Kerr microscope (Germany) provided with electromagnets that allow applying a field in pulsed or continuous modes both parallel and perpendicular to the plane of the films. The polar Kerr effect was used to visualize the magnetic domains. The nucleation of magnetic domains was carried out in a field (16 mT) applied perpendicular to the plane for 2 ms. For a sample with a sublayer thickness of 10 nm, the dynamics of the bias of domain boundaries in crossed magnetic fields of was measured [24]. This technique makes it possible to numerically estimate the constant DMI.

3. Results and discussion

Partial oxidation of the ferromagnetic layer was used to disrupt the symmetry of the upper and lower interfaces necessary for the implementation of DMI. The Pt/Co interface makes it possible to induce perpendicular magnetic anisotropy due to the realization of crystalline stresses in Co and partial hybridization of electronic levels. The combination of a heavy metal with a strong spin-orbit interaction and a ferromagnet makes it possible to induce an interface DMI. Oxidation of the layer leads to a decrease in the functional layer of Co due to the incorporation of oxygen atoms into the surface and, thereby, increases the energy of perpendicular magnetic anisotropy by reducing the contribution of the volumetric anisotropy constant ($K_v = -\frac{\mu_0 M_S^2}{2} + K_{\text{MCA}}$, where $K_{\text{shape}} = -\frac{\mu_0 M_S^2}{2}$ are the constants of shape anisotropy, K_{MCA} are the constants of magnetocrystalline anisotropy [25–26] compared with the contribution of the constant of surface anisotropy).

According to studies, a structurally continuous Pt layer on a SiO_2 substrate is formed with a thickness of about 4 nm [27]. Partial oxidation of the 1 nm thick layer of Co serves to prevent direct contact between Co and Pt.

Structural studies have shown that Bragg peaks corresponding to Pt(111) are observed for all samples. Peak intensity of volumetric pure platinum $2\theta = 39.239$ [28]. In our case, the spectral line is shifted along the axis of angles 2θ and is fixed in the range from 39.401 to 39.933. This indicates the presence of crystalline stresses in the film associated with deformation at the interfaces, and the formation of a Pt-Co alloy at the interface cannot be ruled out.

The average grain size is calculated using the Scherrer formula [29]:

$$d = \frac{K\lambda}{\beta \cos\theta}, \tag{1}$$

where d is the average crystallite size; K is the dimensionless particle shape coefficient (Scherrer constant) equal to 0.94; λ is the X-ray wavelength (0.154 nm); β is the integral broadening (in radians and units 2θ); θ is the diffraction angle (Bragg angle in degrees).

According to the results of the analysis of X-ray spectra, the formation of distinguishable crystalline grains begins at a thickness of Pt $t_{\text{Pt}} > 4$ nm (Figure 1, *a*). The increase in the average platinum grain size is characterized by an almost linear relationship up to a thickness of 10 nm, after which the slope of the curve decreases, which may indicate the completion of coalescence processes and further grain growth in the film plane. According to X-ray reflectometry data, the roughness also increases with the thickness of the Pt layer, which indicates the development of the island structure of the film (Figure 2, *b*).

Figure 1, *b* shows the dependences of the magnetic moment on the thickness of the sublayer. Obviously, at small Pt thicknesses, the increase in the magnetic moment is due to the gradual formation of a continuous Pt/Co interface and a decrease in the areas where Co borders the amorphous SiO_2 substrate. A further increase in the magnetic moment is associated with an increase in the average grain size, which contributes to an increase in the coherent interface area of Pt/Co. The difference between the slope of the graphs for the oxidized and non-oxidized series can be explained by the appearance of induced magnetization in the Pt boundary layer at the Co interface due to the proximity effect [30]. The approximately two-fold change in slope is due to the presence of two Pt/Co and Co/Pt interfaces in the non-oxidized samples.

According to the results of STM measurements (Figure 2, *a*) of the Pt (10 nm) layer, the film grows by an island mechanism. The RMS roughness of the layer is $R_{\text{RMS}} = 0.2$ nm, the average roughness is $R_a = 0.15$ nm. The profile showed islands of the order of 0.8–1 nm, which is consistent with the roughness readings obtained by X-ray diffraction.

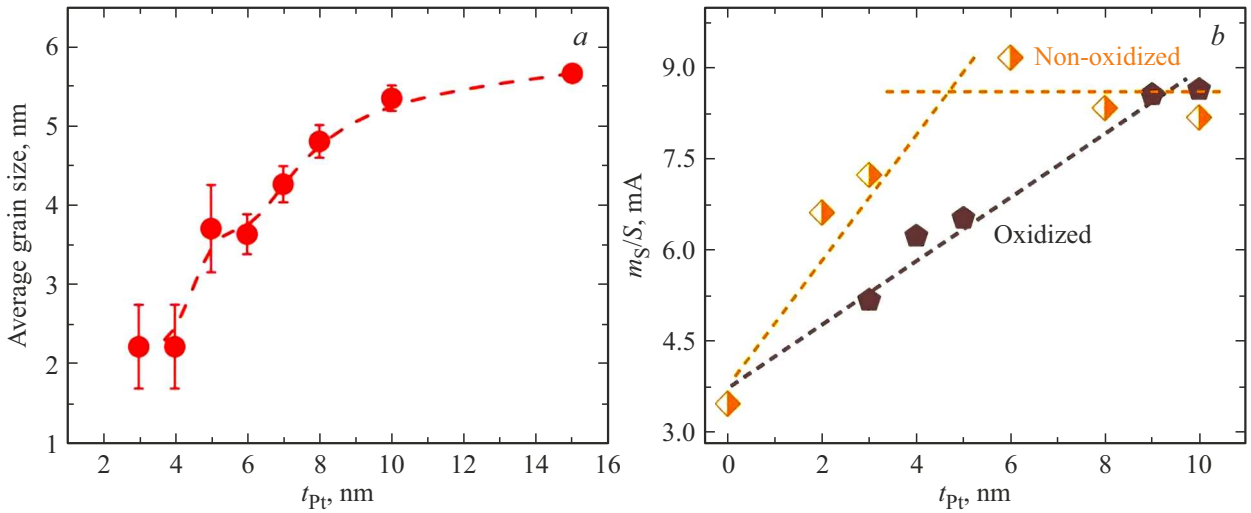

Figure 1. Thickness dependences (a) of the average grain size for the Pt/Co/CoO series (b) of the reduced magnetic moment of Co for the Pt/Co/Pt and Pt/Co/CoO systems.

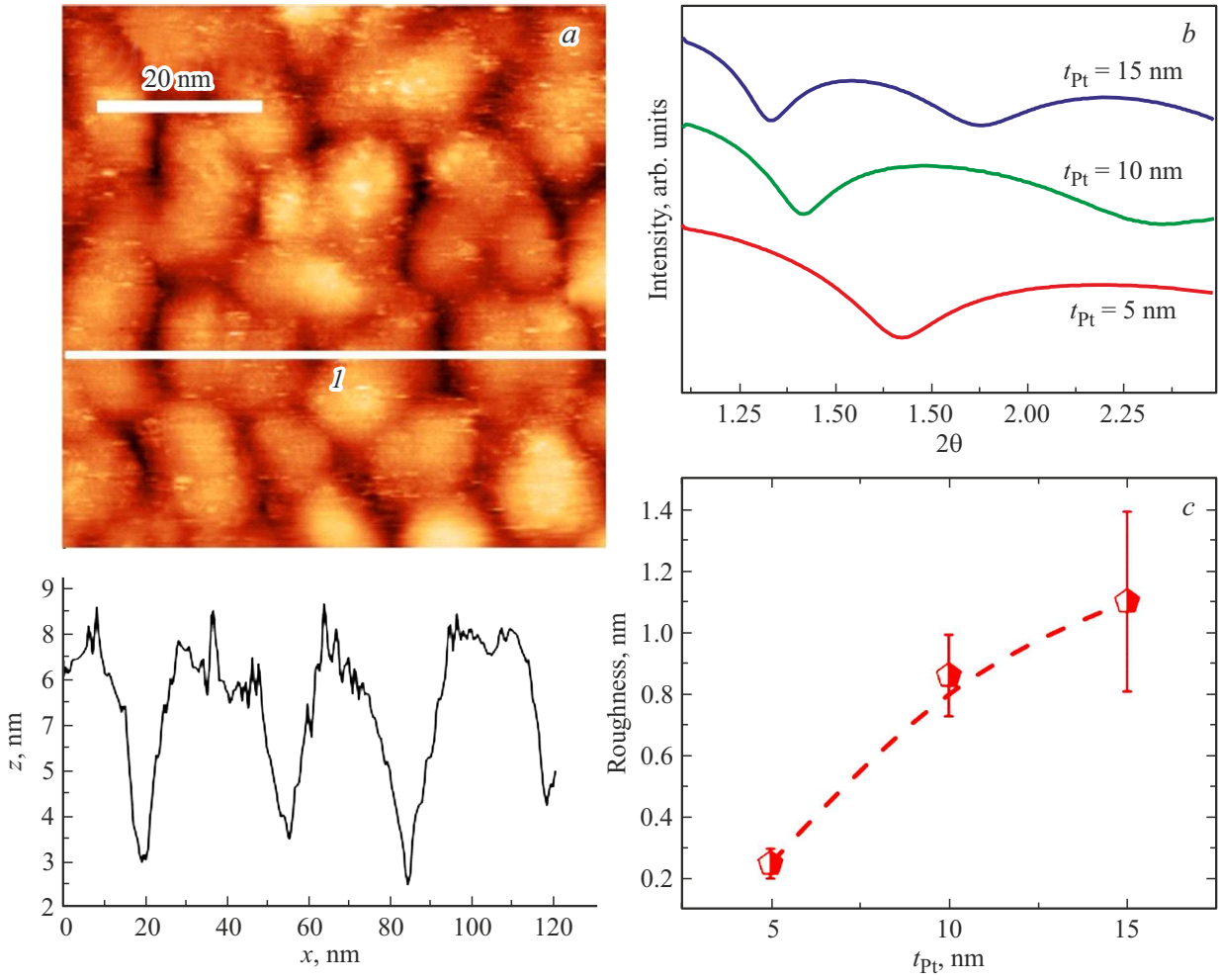

Figure 2. Surface morphology of the Pt layer: a — STM images of SiO_2/Pt(10 nm); b — small-angle diffraction spectra; c — dependence of roughness on Pt thickness, based on the spectra.

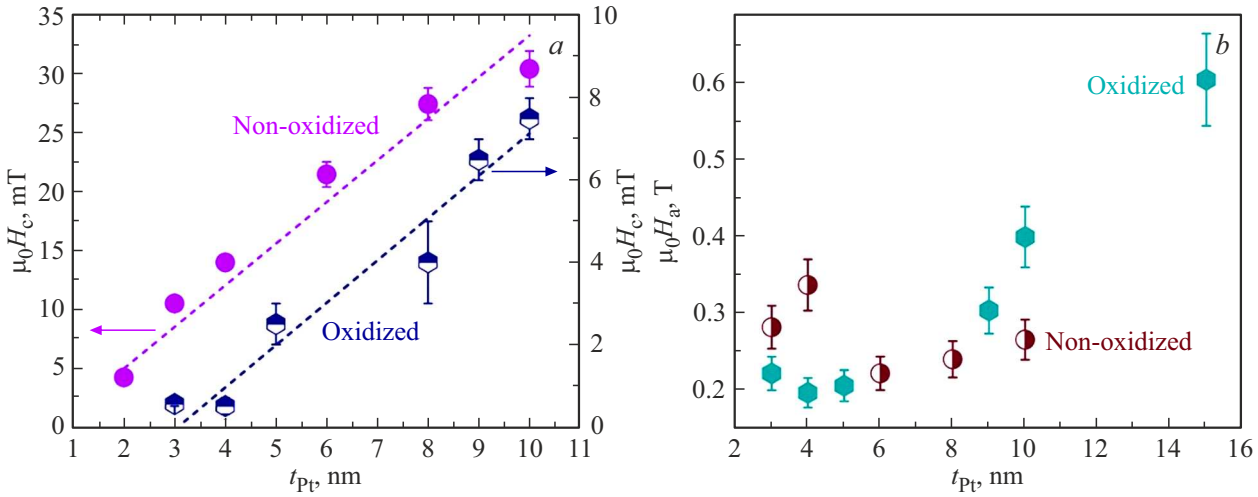

Figure 3. Magnetic characteristics depending on the thickness of the Pt sublayer for Pt/Co/Pt and Pt/Co/CoO/Pt systems *a* — coercive force, *b* — anisotropy fields.

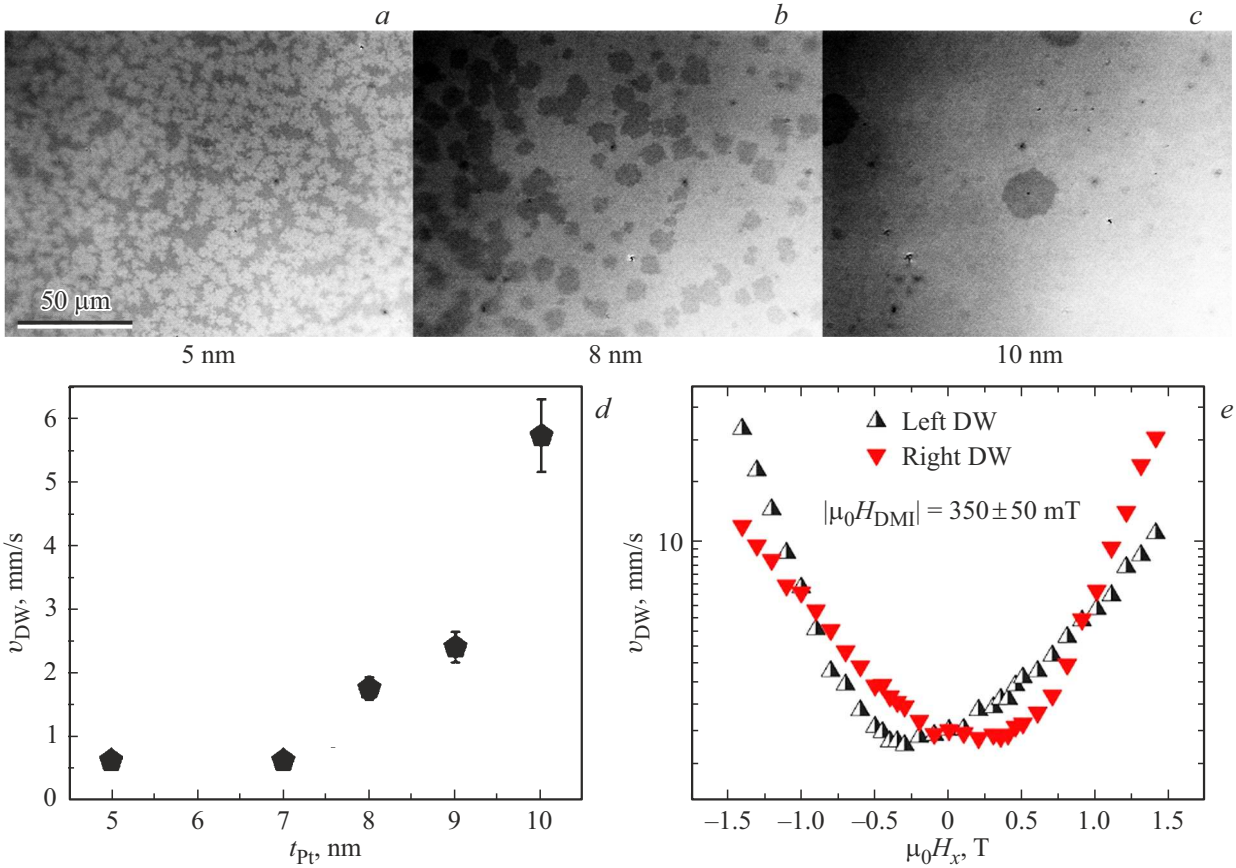

Figure 4. Results of the domain structure study: Kerr images of the domain structure during domain origin for $t_{Pt} = 5$ nm (*a*), $t_{Pt} = 8$ nm (*b*), $t_{Pt} = 10$ nm (*c*); *d* — dependence of the average domain growth rate on the Pt thickness for the Pt/Co/CoO/Pt system in case of application of a short-term pulse of a magnetic field directed perpendicular to the film plane; *e* — the dependence of the velocities of the domain boundaries v_{DW} on the external magnetic field applied in the sample plane H_x as a result of the action of a pulse of a perpendicularly directed field H_z.

All the films obtained exhibit perpendicular magnetic anisotropy, the energy of which increases with increasing thickness of Pt. The dependence of the anisotropy field on the thickness of Pt is shown in Figure 3, *b* for Pt/Co/CoO/Pt and Pt/Co/Pt.

The coercive force in Figure 3, *a* increases linearly for both oxidized and non-oxidized samples, and the dependence is sharper for Pt/Co/Pt films. Oxidized Pt/Co/CoO/Pt films exhibit significantly lower H_c values and a smoother change in it, which can be explained by the diffusion of oxygen atoms into the film volume. The effect of the lower Pt/Co interface on the coercive force can be considered the same for both series, therefore, only the upper interface can be considered responsible for changing the slope of the thickness dependences.

In the images of the domain structure obtained by Kerr microscopy in a field of 16 mT applied perpendicular to the film plane during a short pulse with a width of 20 ms, it is observed that at small thicknesses of the Pt sublayer, the average domain size is relatively small, but the density of the nucleation centers of the domains is relatively large, Figure 4, *a*. This behavior is associated with low anisotropy energy at small thicknesses of the Pt sublayer due to the presence of weakly ordered regions in the Co layer. As the thickness of the sublayer increases (Pt 8 nm), the density of the nucleation centers of the domains decreases, the average size of the domains increases, the anisotropy energy gradually increases due to the formation of a sharper interface and increasing stresses at the Pt/Co boundary caused by an increase in the size of the Pt grain, and, accordingly, the contact area of the materials on grain surfaces. A further increase in thickness leads to a sharp decrease in the density of the nucleation centers of domains due to an increase in the energy of magnetic anisotropy. The average rate of domain nucleation, depending on the thickness of the platinum sublayer, is shown in Figure 4, *b*.

The dynamics of the movement of domain boundaries was measured only for a sample corresponding to a thickness of Pt$t_{\mathrm{Pt}} = 10$ nm due to the high density of domains. The type of dependence of the speeds of movement of the domain boundaries (left and right) on the external planar field in Figure 4, *c* indicates the presence of DMI. The velocity minima correspond to the value of the internal effective Dzyaloshinskii-Moriya field H_{DMI}, which is equal in magnitude but opposite in sign. Based on H_{DMI}, the modulus of the DMI constant $|D_{\mathrm{eff}}|$ can be calculated using the formula:

$$|D_{\mathrm{eff}}| = \mu_0 M_S |H_{\mathrm{DMI}}| \sqrt{\frac{A_{\mathrm{ex}}}{K_{\mathrm{eff}}}}, \qquad (2)$$

where M_s and A_{ex} — saturation magnetization and exchange energy, respectively ($M_{S(\mathrm{Co})} = 1.1$ A/m, $A_{\mathrm{ex}} = 2.8 \cdot 10^{-11}$ J/m), which are taken from tabular values, K_{eff} — effective anisotropy constant, the anisotropy field is taken from experimental values.

The Dzyaloshinskii-Moriya constant for the system SiO_2/Pt(10 nm)/Co/CoO/Pt(5 nm)$D_{\mathrm{eff}} = 0.37$ mJ/m^2. This value is close to the value measured in similar Pd(2 nm)/Co(0.8 nm)/CoO/Pd(3 nm) systems [22]. For comparison, in structures using MgO, AlO_x as an oxide metal, the DMI constant is significantly higher ($D_{\mathrm{eff(MgO)}}$=3 mJ/m^2, $D_{\mathrm{eff}(AlO_x)}$=0.87 mJ/m^2) [31], however, they require the use of sources for sputtering MgO, AlO_x, which somewhat complicates the technology of obtaining heterostructures.

4. Conclusion

The conducted studies have shown that the thickness of Pt in the Pt/Co/CoO film system significantly affects their structural and magnetic properties. With an increase in the size of the crystallite of the Pt sublayer, the values of the coercive force, magnetic moment, anisotropy field, and the nucleation rate of domains increase. In such a system, DMI can manifest itself, and for the SiO_2/Pt(10 nm)/Co/CoO/Pt system, the DMI constant is $D_{\mathrm{eff}} = 0.37$ mJ/m^2.

The established patterns can be used to optimize the parameters of materials used in magnetic recording and spintronics devices.

Acknowledgments

Alexey Gavriilovich Kozlov would like to thank the Russian Science Foundation for the financial support of the research (project No. 24-72-00162). Kuznetsova Maria Alekseevna, Prikhodchenko Alyona Vitalievna, Turpak Alexander Alekseevich, Chernousov Nikolay Nikolaevich would like to thank the state assignment No. FZNS-2023–0012.

References

[1] Q.L. Lv, J.W. Cai, H.Y. Pan, B.S. Han. Appl. Phys. Express **3**, *9*, 093003 (2010).
[2] M. Li, Q. Li, S. Zhang, J. Fu, F. Gu, W. Ma, H. Shi, G. Yu. Vacuum **205**, 111410 (2022).
[3] Z. Chen, C. Pan, N. Wang, M. Qiu, T. Lin, J. Liu, S. Li, P. Han, J. Shi, K. Ando, H. An. J. Magn. Magn. Mater. **507**, 166822 (2020).
[4] M. Schott, L. Ranno, H. Béa, C. Baraduc, S. Auffret, A. Bernand-Mantel. J. Magn. Magn. Mater. **520**, 167122 (2021).
[5] K.-W. Lin, J.-Y. Guo, S. Kahwaji, S.-C. Chang, H. Ouyang, J. van Lierop, N.N. Phuoc, T. Suzuki. Phys. Status Solidi A **204**, *12*, 3970 (2007).
[6] D.I. Anyfantis, C. Ballani, N. Kanistras, A. Barnasas, I. Tsiaoussis, G. Schmidt, E.Th. Papaioannou, P. Poulopoulos. Materials **16**, *4*, 1378 (2023).
[7] S. Parkin, S.-H. Yang. Nat. Nanotechnol. **10**, *3*, 195 (2015).
[8] K. Gu, Y. Guan, B.K. Hazra, H. Deniz, A. Migliorini, W. Zhang, S.S.P. Parkin. Nat. Nanotechnol. **17**, *10*, 1065 (2022).
[9] J. Lenz, S. Edelstein. IEEE Sens. J. **6**, *3*, 631 (2006).
[10] T. Blachowicz, A. Ehrmann. Molecules **25**, *11*, 2550 (2020).

[11] H. Yang, A. Thiaville, S. Rohart, A. Fert, M. Chshiev. Phys. Rev. Lett. **115**, *26*, 267210 (2015).
[12] A.V. Zdoroveishcheva, O.V. Vikhrovaa, P.B. Demina, M.V. Dorokhina, A.V. Kudrina, A.G. Temiryazev, M.P. Temiryazeva. FTT **61**, *9*, 1628 (2019). (in Russian).
[13] A.S. Samardak, A.V. Davydenko, A.G. Kolesnikov, A.Yu. Samardak, A.G. Kozlov, Bappaditya Pal, A.V. Ognev, A.V. Sadovnikov, S.A. Nikitov, A.V. Gerasimenko, In Ho Cha, Yong Jin Kim, Gyu Won Kim, Oleg A. Tretiakov, Young Keun Kim. NPG Asia Mater. **12**, *1*, 51 (2020).
[14] K. Kyuno, R. Yamamoto, S. Asano. J. Phys. Soc. Jpn. **61**, *6*, 2099 (1992).
[15] C. Chappert, P. Bruno. J. Appl. Phys. **64**, *10*, 5736 (1988).
[16] M. Kisielewski, A. Maziewski, M. Tekielak, J. Ferré, S. Lemerle, V. Mathet, C. Chappert. J. Magn. Magn. Mater. **260**, *1−2*, 231 (2003).
[17] S. Bandiera, R.C. Sousa, B. Rodmacq, B. Dieny. IEEE Magn. Lett. **2**, 3000504 (2011).
[18] S. Chen, D. Li, B. Cui, L. Xi, M. Si, D. Yang, D. Xue. J. Phys. D: Appl. Phys. **51**, *9*, 095001 (2018).
[19] A.W.J. Wells, P.M. Shepley, C.H. Marrows, T.A. Moore. Phys. Rev. B **95**, *5*, 054428 (2017).
[20] R. Lavrijsen, D.M.F. Hartmann, A. van den Brink, Y. Yin, B. Barcones, R.A. Duine, M.A. Verheijen, H.JḾ. Swagten, B. Koopmans. Phys. Rev. B **91**, *10*, 104414 (2015).
[21] N.S. Gusev, Yu.A. Dudin, A.V. Sadovnikov, M.V. Sapozhnikov. FTT **63**, *9*, 1263 (2021). (in Russian).
[22] A.G. Kozlov, A.V. Davydenko, L.L. Afremov, I.G. Iliushin, V.N. Kharitonov, P.S. Mushtuk, E.V. Tarasov, A.A. Turpak, A.F. Shishelov, N.N. Chernousov, M.E. Letushev, A.V. Sadovnikov, A.B. Khutieva, A.V. Ognev, A.S. Samardak. ACS Appl. Electron. Mater. **6**, 4928 (2024).
[23] A.G. Kozlov, A.F. Shishelov, A.A. Turpak, M.A. Kuznetsova, A.V. Prikhodchenko, A.V. Davydenko, E.V. Tarasov, N.N. Chernousov, A.V. Ognev, A.S. Samardak. J. Magn. **29**, *1*, 143 (2024).
[24] S.G. Je, D.H. Kim, S.C. Yoo, B.C. Min, K.J. Lee, S.B. Choe. Phys. Rev. B **88**, *21*, 214401 (2013).
[25] A.V. Davydenko, A.G. Kozlov, A.V. Ognev, M.E. Stebliy, A.S. Samardak, K.S. Ermakov, A.G. Kolesnikov, L.A. Chebotkevich. Phys. Rev. B **95**, *6*, 064430 (2017).
[26] L.A. Chebotkevich, A.V. Ognev, B.N. Grudin. FTT **46**, *8*, 1449 (2004). (in Russian).
[27] J.S. Agustsson, U.B. Arnalds, A.S. Ingason, K.B. Gylfason, K. Johnsen, S. Olafsson, J.T. Gudmundsson. J. Phys.: Conf. Ser. **100**, *8*, 082003 (2008).
[28] I. Zrinski, A. Minenkov, C. Cancellieri, R. Hauert, C.C. Mardare, J.P. Kollender, L.P.H. Jeurgens, H. Groiss, A.W. Hassel, A.I. Mardare. Appl. Mater. Today **26**, 101270 (2022).
[29] A.L. Patterson. Phys. Rev. **56**, *10*, 978 (1939).
[30] R.M. Rowan-Robinson, A.A. Stashkevich, Y. Roussigné, M. Belmeguenai, S.-M. Chérif, A. Thiaville, T.P.A. Hase, A.T. Hindmarch, D. Atkinson. Sci. Rep. **7**, *1*, 16835 (2017).
[31] M. Kuepferling, A. Casiraghi, G. Soares, G. Durin, F. Garcia-Sanchez, L. Chen, G. Carlotti. Rev. of Mod. Phys. **95**, *1*, 015003 (2023).

Translated by A.Akhtyamov